J. Serb. Chem. Soc. *64*(5–6)317-340(1999)
JSCS-2673

UDC 66.022.03:543.251:621.793
Review paper

REVIEW

Mass transfer during electrodeposition of metals at a periodically changing rate

MIODRAG D. MAKSIMOVIĆ and KONSTANTIN I. POPOV

Faculty of Technology and Metallurgy, University of Belgrade, P.O.Box 3503, YU–11120 Belgrade, Yugoslavia

(Received 2 February 1999)

Key words: mass-transfer, electrodeposition, reversing current, pulsating current, alternating current superimposed on direct current, pulsating overpotential.

1. INTRODUCTION

It has been known for a relatively long time that the application of a periodically changing current in plating practice leads to improvements in the quality of electrodeposits. Three types of current variation have been found useful: a reversing current (RC); a pulsating current (PC); and a sinusoidal, alternating current superimposed on a direct current (AC).[1–15] In recent years, the beneficial effects of pulsating overpotential (PO) have also been discussed.[4] Even though this kind of electrodeposition at a periodically changing rate (EPCR) is important from a theoretical point of view and offers a variety of experimental possibilities, it is not as yet, frequently used in plating practice.

The mass transfer during metal electrodeposition at a periodically changing rate is not widely known but it will be treated in details in this paper. It is very

important, because the mass transfer conditions determine the morphology of metal deposits just as in the case of deposition at a constant rate.

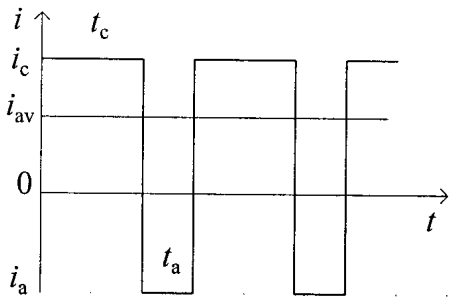

Fig. 1. Waveform of the reversing current.

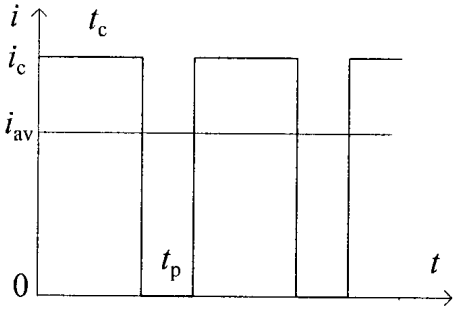

Fig. 2. Pulsatung current.

Reversing current is represented schematically in Fig. 1. It is characterized by the cathodic current density, i_c, and the anodic current density, i_a, as well as by the duration of flow of the current in the cathodic and the anodic direction, t_c and t_a, respectively. Naturally,

$$t_c + t_a = T \tag{1}$$

where T is the full period of the RC wave. The average current density is then given by

$$i_{av} = \frac{i_c t_c - i_a t_a}{t_c + t_a} \tag{2}$$

and for $i_c = i_a = i_A$

$$i_{av} = i_A \frac{1 - r}{1 + r} \tag{3}$$

where

$$r = \frac{t_a}{t_c} \tag{4}$$

RC is used in the second and millisecond range.

Pulsating current consists of a periodic repetition of square pulses. It is similar in shape to RC except for the absence of the anodic component, as is shown in Fig. 2. PC is characterized by the amplitude of the cathodic current, i_c, the cathodic deposition time, t_c (on period), and the time interval t_p in which the system relaxes (off period). The full period, T, is given by

$$t_c + t_p = T \tag{5}$$

and the average current density by

$$i_{av} = \frac{i_c t_c}{t_c + t_p} \tag{6}$$

or

$$i_{av} = \frac{i_c}{1 + p} \tag{7}$$

if

$$p = \frac{t_p}{t_c} \tag{8}$$

Note that rectified sinusoidal AC, especially half-rectified sinusoidal AC, often termed pulsating current in the literature, shows similar effects to those of PC.

Sinusoidal AC superimposed on direct current is represented in Fig. 3. It is characterized by i_{dc}, i_p, and the frequency, which is usually 50 or 60 Hz. The resultant is termed an asymmetric sinusoidal current. The average current is equal to i_{dc}. At given anodic DC values, three different types of current can be obtained, which can be denoted as follows: $i_p < i_{dc}$ "rippling current"; $i_p = i_{dc}$,"pulsating curren"; $i_p > i_{dc}$, "current with an anodic component". The last type is mainly used in plating practice.

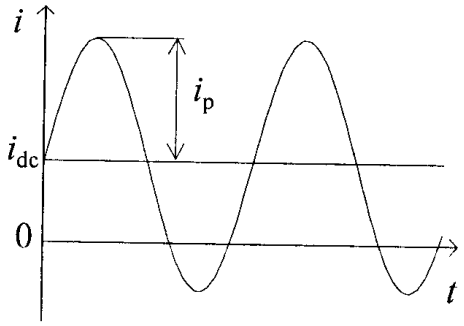

Fig. 3. The shape of the sinusoidal alternating current superimposed on the direct current.

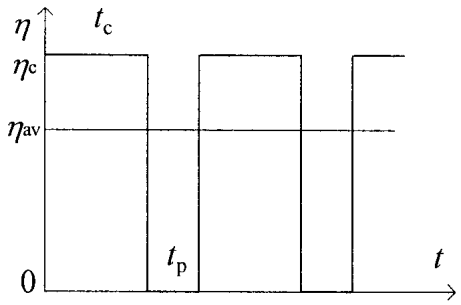

Fig. 4. Square-wave pulsating overpotential waveform.

Pulsating overpotential consists of a periodic repetition of overpotential pulses of different shapes. Square-wave PO is defined in the same way as PC except that the overpotential pulsates between the amplitude value η_A and zero instead of the current density (Fig. 4). Non-rectangular pulsating overpotential is defined by the amplitude of the overpotential, η_A, frequency, and the overpotential waveform.

There are a number of different current and overpotential waveforms used in EPCR,[16–18] the most important of which have been mentioned above.

2. MASS TRANSFER IN THE STEADY STATE PERIODIC CONDITION

Electrodeposition at a periodically changing rate can be described in terms of time and distance-dependent concentrations:

$$\frac{\partial c}{\partial t} = D\frac{\partial^2 c}{\partial x^2} \tag{9}$$

$$c(0,x) = c_0 \tag{10}$$

$$c(t,\delta) = c_0 \tag{11}$$

$$\left|\frac{\partial c}{\partial x}\right|_{x=0} = \frac{i(t)}{zFD} \tag{12}$$

Equations (9) to (12) are solved for different $i(t)$ and the solutions applied to different types of problems.[16–41]

2.1. Reversing current

For the periodic reverse current the current density $i(t)$ is a periodic function of time given by[36]

$$i(t) = \begin{cases} i_c, & \text{for } mT < t \le [m + 1/(r+1)]T \\ -i_a & \text{for } [m + 1/(r+1)]T < t \le (m+1)T \end{cases} \tag{13}$$

$m = 0, 1, 2,\ldots$

Millisecond range. For $i(t)$ given by Eq. (13), the solution of Eqs. (9) to (12) is given by

$$c(x,t) = c_0 - \frac{2i_c}{zF\delta}\sum_{k=0}^{\infty}\cos\left[\frac{(2k+1)\pi x}{2\delta}\right]\left\{\int_0^{T/(r+1)}\exp[-\lambda_k(t-\tau)]\,d\tau + \int_T^{T+T/(r+1)}\exp[-\lambda_k(t-\tau)]\,d\tau + \ldots\right.$$
$$\left.\ldots + \int_{mT}^{mT+T/(r+1)}\exp[-\lambda_k(t-\tau)]\,d\tau\right\} + \frac{2i_a}{zF\delta}\sum_{k=0}^{\infty}\cos\left[\frac{(2k+1)\pi x}{2\delta}\right]\left\{\int_{T/(r+1)}^{T}\exp[-\lambda_k(t-\tau)]\,d\tau + \right.$$
$$\left. + \int_{T+T/(r+1)}^{2T}\exp[-\lambda_k(t-\tau)]\,d\tau + \ldots + \int_{mT+T/(r+1)}^{(m+1)T}\exp[-\lambda_k(t-\tau)]\,d\tau\right\} \tag{14}$$

where

$$\lambda_k = \frac{(2k+1)^2\pi^2 D}{4\delta^2} = \frac{(2k+1)^2}{4t_0} \tag{15}$$

and

$$t_0 = \frac{\delta^2}{\pi^2 D} \tag{16}$$

For $t = [m + 1/(r+1)]T$ and $m \to \infty$, *i.e.*, at the end of the cathodic pulses under steady state conditions, the concentration distribution of the depositing ions inside the diffusion layer is given by

$$c_c(x) = c_0 - \frac{8\delta}{\pi^2 zFD} \sum_{k=0}^{\infty} \frac{1}{(2k+1)^2} \cos\frac{(2k+1)\pi x}{2\delta}$$

$$\left\{ i_c \frac{1 - \exp[-\lambda_k T/(r+1)]}{1 - \exp(-\lambda_k T)} - i_a \frac{\exp[-\lambda_k T/(r+1)] - \exp(-\lambda_k T)}{1 - \exp(-\lambda_k T)} \right\} \quad (17)$$

The concentration distribution at the end of the anodic pulses under the same conditions, *i.e.* for $t = (m+1)T$, $m \to \infty$, is given by

$$c_a(x) = c_0 - \frac{8\delta}{\pi^2 zFD} \sum_{k=0}^{\infty} \frac{1}{(2k+1)^2} \cos\frac{(2k+1)\pi x}{2\delta}$$

$$\left\{ i_c \frac{\exp[-\lambda_k rT/(r+1)] - \exp(-\lambda_k T)}{1 - \exp(-\lambda_k T)} - i_a \frac{1 - \exp[-\lambda_k rT/(r+1)]}{1 - \exp(-\lambda_k T)} \right\} \quad (18)$$

It is easy to show that, for a sufficiently long period T ($T > t_o$), the system behaves as under DC conditions. For $T \to \infty$ Eqs. (17) and (18) become

$$\lim_{T\to\infty} c_c(x) = c_0 - \frac{i_c}{zFD}(\delta - x) \quad (19)$$

and

$$\lim_{T\to\infty} c_a(x) = c_0 - \frac{i_a}{zFD}(\delta - x) \quad (20)$$

On the other hand, for $T \to 0$ ($T << t_0$)

$$\lim_{T\to 0} c_c(x) = \lim_{T\to 0} c_a(x) = c(x) = c_0 - \frac{\delta - x}{zFD} \frac{i_c - r\, i_a}{r+1} = c_0 - \frac{\delta - x}{zFD} i_{av} \quad (21)$$

for $0 \le x \le \delta$

The concentration distribution inside the diffusion layer at the end of cathodic and anodic pulses under steady state conditions, calculated using Eqs. (17) and (18) and the following set of parameters $\delta = 10^{-2}$ cm, $D = 10^{-5}$ cm^2 s^{-1} and $t_0 = 1$ s, is given in Figs. 5 – 9 for different reversing regimes. At sufficiently large x/δ, the concentration distribution does not depend on time.[42] At x/δ close to the electrode, it is time dependent and the upper and lower parts of the curves correspond to the end of the anodic and the cathodic times, respectively.

It can be seen from Fig. 5 that, at lower periods of the RC wave, the concentration distribution is closer to one described by Eq. (21) for $T \to 0$. It can also be seen from Fig. 6 and Fig. 7 that, with other parameters, the same the distribution is closer to that given by Eq. (21) at lower r and i_{av} values.

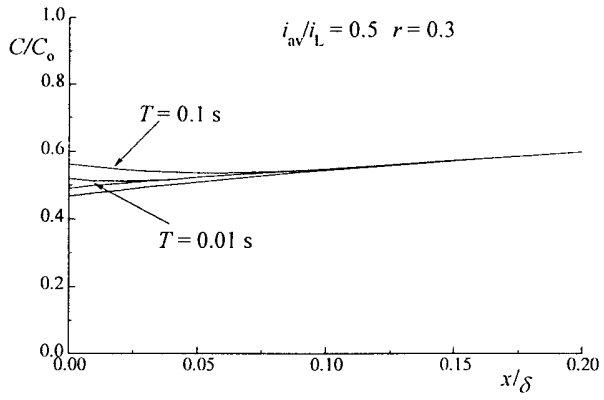

Fig. 5. The effect of the period of the RC wave on the concentration distribution inside the diffusion layer (From Maksimović and Popov[42]).

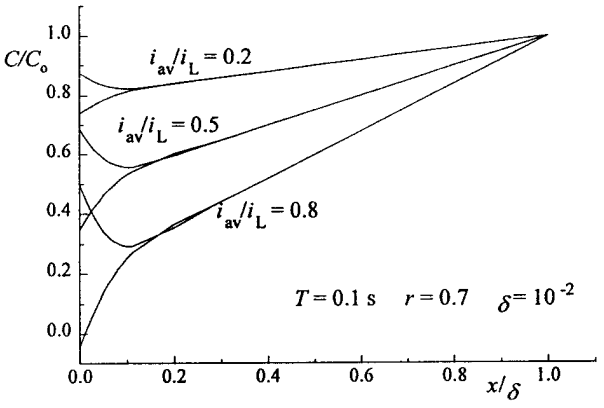

Fig. 6. The effect of the average current density on the concentration distribution inside the diffusion layer. (From Maksimović and Popov[42]).

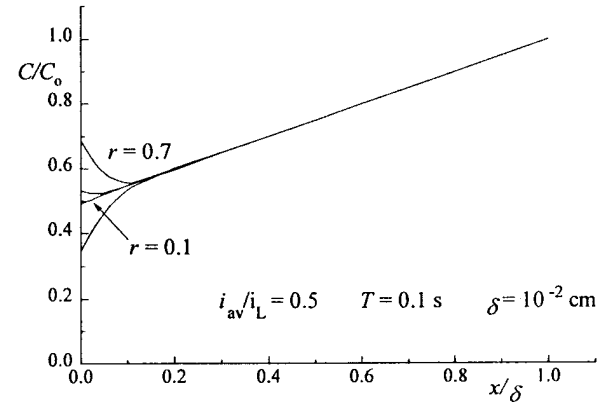

Fig. 7. The effect of the anodic to cathodic time ratio on the concentration distribution inside the diffusion layer. (From Maksimović and Popov[42]).

At $i_{av} = 0$, concentration polarization practically does not exists up to $i_A \approx i_L$, as is illustrated by Fig. 8.

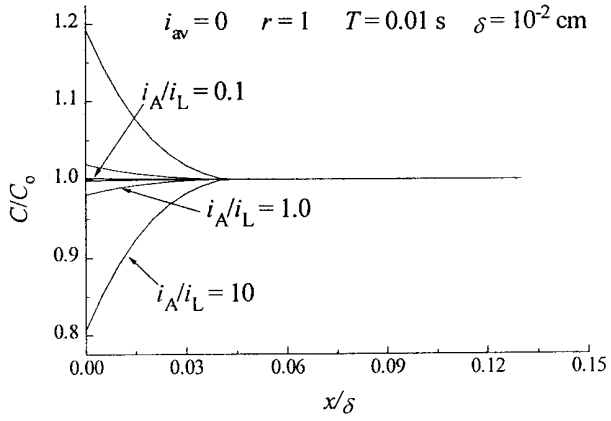

Fig. 8. The effect of the current amplitude on the concentration distribution inside the diffusion layer. (From Maksimović and Popov[42]).

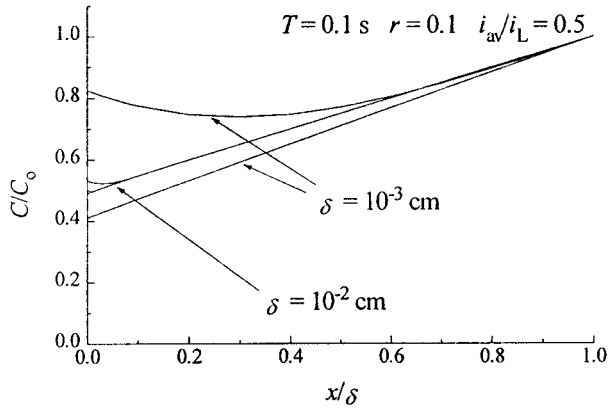

Fig. 9. The effect of the diffusion layer thickness on the concentration distribution inside the diffusion layer. (From Maksimović and Popov[42]).

Finally, the effect of the diffusion layer thickness is shown in Fig. 9. It follows from Eqs. (15) – (18) that the frequency of pulsation and diffusion layer thickness are related by the equation

$$\frac{T}{\delta^2} = \text{const.} \tag{22}$$

to produce the same effect on the concentration distribution inside the diffusion layer.

For $x = 0$, Eqs. (17) and (18) can be rewritten in the form

$$c_c = c_0 - \frac{8\delta}{\pi^2 zFD} \sum_{k=0}^{\infty} \frac{1}{(2k+1)^2} \left\{ i_c \frac{1 - \exp[-\lambda_k T/(r+1)]}{1 - \exp(-\lambda_k T)} - i_a \frac{\exp[-\lambda_k T/(r+1)] - \exp(-\lambda_k T)}{1 - \exp(-\lambda_k T)} \right\} \tag{23}$$

and (24)

$$c_a = c_0 - \frac{8\delta}{\pi^2 zFD}\sum_{k=0}^{\infty}\frac{1}{(2k+1)^2}\left\{i_c\frac{\exp[-\lambda_k rT/(r+1)] - \exp(-\lambda_k t)}{1-\exp(-\lambda_k T)} - i_a\frac{\exp[-\lambda_k T/(r+1)]}{1-\exp(-\lambda_k T)}\right\}$$

and Eqs. (19)–(21) in the form

$$\lim_{T\to\infty} c_c = c_0 - \frac{\delta i_c}{zFD} \tag{25}$$

$$\lim_{T\to\infty} c_a = c_0 - \frac{\delta i_a}{zFD} \tag{26}$$

and

$$\lim_{T\to 0} c_c = \lim_{T\to 0} c_a = c_s = c_0 - \frac{\delta}{zFD}\frac{i_c - r\,i_a}{r+1} = c_0 - \frac{\delta}{zFD} i_{av} \tag{27}$$

Second range. For T close to t_0, the behaviour of the system under RC conditions has to be analyzed using Eq. (24). In this case, the distribution of the concentration inside the diffusion layer at the end of the anodic pulse is close to that given by Eq. (10). It follows from Eq. (24) that this will happen at[36,43]

$$c_a = c_0 \tag{28}$$

or

$$\sum_{k=0}^{\infty}\frac{1}{(2k+1)^2}\left\{i_c\frac{\exp[-\lambda_k rT/(r+1)] - \exp(-\lambda_k T)}{1-\exp(-\lambda_k T)} - i_a\frac{1-\exp[-\lambda_k rT/(r+1)]}{1-\exp(-\lambda_k T)}\right\} = 0 \tag{29}$$

Obviously, r can be obtained by computer calculation from Eq. (29).

On the other hand, it is known[36,52] that for $rT/(r+1) \geq 1.5t_0$, the series in Eq. (29) can be approximated using only the first term ($k = 0$). Hence, for $i_c = i_a$,

$$\exp\left(-\frac{r}{r+1}\frac{T}{4t_0}\right) - \exp\left(-\frac{T}{4t_0}\right) = 1 - \exp\left(-\frac{r}{r+1}\frac{T}{4t_0}\right) \tag{30}$$

or

$$r = \frac{\dfrac{4t_0}{T}\ln\dfrac{2}{1+\exp(-T/4t_0)}}{1-\dfrac{4t_0}{T}\ln\dfrac{2}{1+\exp(-T/4t_0)}} \tag{31}$$

It is easy to show that for $T = 3t_0$, $r = 0.7$ and for $T = 16t_0$, $r = 0.2$ by assuming that for $T > 3t_0$, Eq. (30) is valid and that at $T > 16t_0$, the system behaves as under DC conditions. The optimum ratio t_c/t_a is given by

$$1.5 \leq t_c/t_a \leq 5 \tag{32}$$

for periods T such that

$$3t_0 \leq T \leq 16t_0 \tag{33}$$

and the optimum t_c and t_a for a given T, calculated using Eq. (31), are shown in Fig. 10.

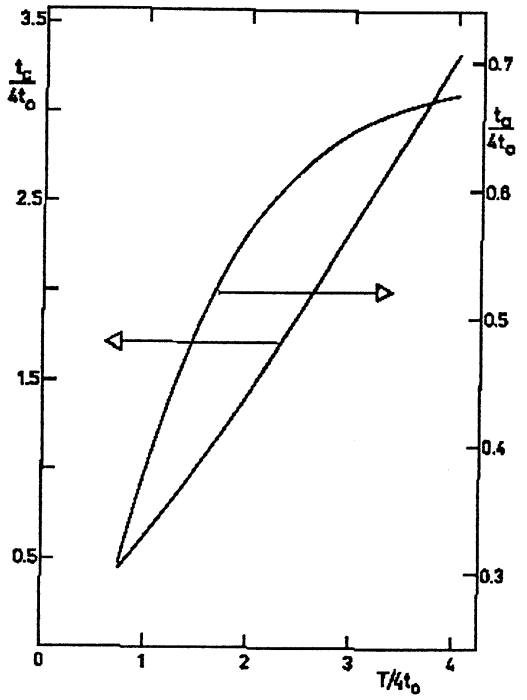

Fig. 10. $t_c/4t_0$ and $t_a/4t_0$ as a function of $T/4t_0$. (From Popov and Maksimović[43]).

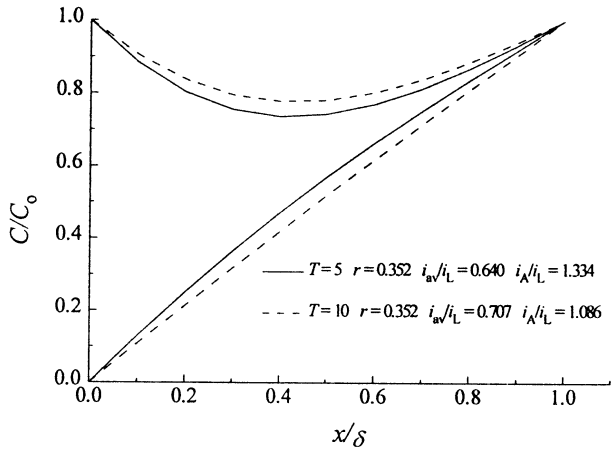

Fig. 11. The concentration distribution inside the diffusion layer at the end of the anodic (upper) and the cathodic (lower) times. Calculated by computer using Eqs. (17) and (29).

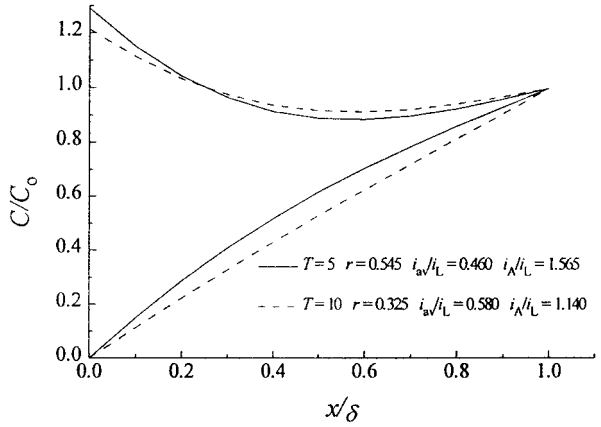

Fig. 12. The concentration distribution inside the diffusion layer at the end of the anodic (upper) and the cathodic (lower) times. Calculated by computer using Eqs. (17) and (31).

In Fig. 11. and Fig. 12, the concentration distribution at the end of the cathodic and anodic pulses for optimum current wave shapes are shown, calculated by computer (Fig. 10.) and by using Eq. (33) if $t_0 = 1$ s for $\delta = 10^{-2}$ cm and $D = 10^{-5}$ cm^2 s^{-1} (Fig. 11.). It is seen that the approximation used is satisfactory. A good agreement between the shape and the frequency of the RC calculated in this way and literature data is obtained, because in practically all cases

$$1 \text{ s} \leq T \leq 30 \text{ s} \tag{34}$$

according to Bakhvalov.[3]

For periods T:

$$3\, t_0 \leq \mathrm{T} \leq 16\, t_0 \tag{35}$$

It is obvious that, because of Eq. (35) and the dependence of t_0 on the diffusion layer thickness, in strongly stirred solutions the period T must be considerably smaller.

2.2. Pulsating current

For $i(t)$ given by

$$i(t) = \begin{cases} i_c, & \text{for } mT < t \leq [m + 1/(p+1)]T \\ 0, & \text{for } [m + 1/(p+1)]T < t \leq (m+1)T \end{cases} \tag{36}$$

i.e. for pulsating current,' solution of Eqs. (9) to (12) is given by

$$c(x,t) = c_0 - \frac{2i_c}{zF\delta} \sum_{k=0}^{\infty} \cos\left[\frac{(2k+1)\pi x}{2\delta}\right]$$

$$\left\{ \int_0^{T/(p+1)} \exp\left[-\lambda_k (t-\tau)\right] d\tau + \int_T^{T+T/(p+1)} \exp\left[-\lambda_k (t-\tau)\right] d\tau + \ldots + \int_{mT}^{mT+T/(p+1)} \exp[-\lambda_k (t-\tau)]\, d\tau \right\} \tag{37}$$

For $t = [m + 1/(p+1)]T$, *i.e.*, at the end of pulses, Eq. (37) can be rewritten as

$$c\left\{x, \left(m + \frac{1}{p+1}\right)T\right\} = c_0 - \frac{8\delta\, i_c}{\pi^2\, zFD} \sum_{k=0}^{\infty} \frac{1}{(2k+1)^2} \cos\frac{(2k+1)\pi x}{2\delta}$$
$$\left\{\exp(-\lambda_k T) - \exp\left[-\lambda_k\left(T + \frac{T}{p+1}\right)\right] + ... + 1 - \exp\left(-\frac{\lambda_k T}{p+1}\right)\right\} \quad (38)$$

In steady state conditions

$$c_{on}(x) = \lim_{m\to\infty} c\left\{x, \left(m + \frac{1}{p+1}\right)T\right\} =$$

$$= c_0 - \frac{8\delta\, i_c}{\pi^2\, zFD} \sum_{k=0}^{\infty} \frac{1}{(2k+1)^2} \cos\frac{(2k+1)\pi x}{2\delta} \frac{1 - \exp[-\lambda_k T/(p+1)]}{1 - \exp(-\lambda_k t)} \quad (39)$$

For $t = (m+1)T$, *i.e.*, at the end of pauses, Eq. (37) can be rewritten in the form

$$c[x, (m+1)T] = c_0 - \frac{8\delta i_c}{\pi^2\, zFD} \sum_{k=0}^{\infty} \frac{1}{(2k+1)^2} \cos\frac{(2k+1)\pi x}{2\delta} \cdot \left\{\exp\left[-\lambda_k\left((m+1)T + \frac{T}{p+1}\right)\right] - \right.$$
$$\left. - \exp[-\lambda_k (m+1)T] + \ldots + \exp\left[-\lambda_k\left(T - \frac{T}{p+1}\right)\right] - \exp(-\lambda_k T)\right\} \quad (40)$$

In steady state conditions

$$c_{off}(x) = \lim_{m\to\infty} c[x, (m+1)T] =$$

$$= c_0 - \frac{8\delta\, i_c}{\pi^2 zFD} \sum_{k=0}^{\infty} \frac{1}{(2k+1)^2} \cos\frac{(2k+1)\pi x}{2\delta} \frac{\exp\{-\lambda_k[T - T/(p+1)]\} - \exp(-\lambda_k T)}{1 - \exp(-\lambda_k T)} \quad (41)$$

For $T \to \infty$ Eqs. (39) and (41) becomes

$$\lim_{T\to\infty} c_{on}(x) = c_0 - \frac{i_c}{zFD}(\delta - x) \quad (42)$$

and

$$\lim_{T\to\infty} c_{off}(x) = c_0 \quad (43)$$

while for $T \to 0$

$$\lim_{T\to 0} c_{on}(x) = \lim_{T\to 0} c_{off}(x) = c(x) = c_0 - \frac{\delta - x}{zFD} \frac{i_c}{p+1} \quad (44)$$

At the same time for $x = 0$, Eqs. (39) and (41) becomes

$$c_{on} = c_0 - \frac{8\delta i_c}{\pi^2 zFD} \sum_{k=0}^{\infty} \frac{1}{(2k+1)^2} \frac{1 - \exp[-\lambda_k T/(p+1)]}{1 - \exp(-\lambda_k T)} \tag{45}$$

and

$$c_{off} = c_0 - \frac{8\delta i_c}{\pi^2 zFD} \sum_{k=0}^{\infty} \frac{1}{(2k+1)^2} \frac{\exp[-\lambda_k pT/(p+1)] - \exp(-\lambda_k T)}{1 - \exp(-\lambda_k T)} \tag{46}$$

As in the previous case for $T >> t_0$, the system behaves as under DC conditions where

$$\lim_{T\to\infty} c_{on} = c_0 - \frac{\delta i_c}{zFD} \tag{47}$$

and

$$\lim_{T\to\infty} c_{off} = c_0 \tag{48}$$

For $T << t_0$, it follows from Eqs. (45) and (46) that

$$\lim_{T\to 0} c_{on} = \lim_{T\to 0} c_{off} = c_s = c_0 - \frac{\delta i_c}{zFD} \frac{1}{p+1} \tag{49}$$

It is obvious from Eqs. (2), (4), (7) and (8) and Eqs. (27) and (49) that, in both cases,

$$c_s = c_0 - \frac{\delta i_{av}}{zFD} \tag{50}$$

The concentration distribution inside the diffusion layer at the end of the cathodic pulses and during the pauses in the steady state conditions, calculated using Eqs. (39) and (41) and the already used set of parameters, are given in Figs. 13–16.[45]

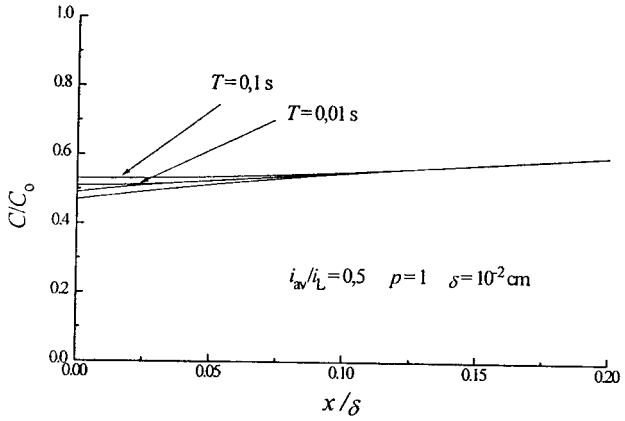

Fig. 13. The effect of the period of the PC wave on the concentration distribution inside the diffusion layer. (From Maksimović and Popov[45]).

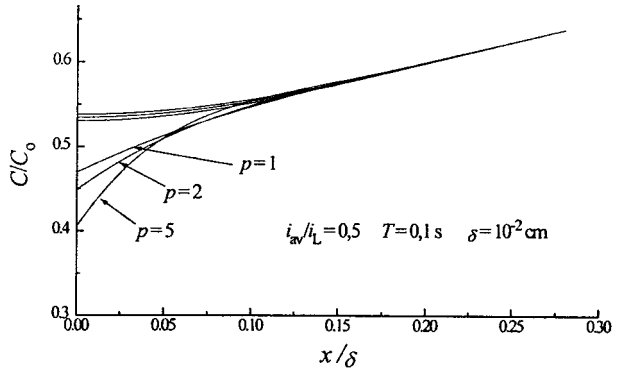

Fig. 14. The effect of the pause to pulse ratio on the concentration distribution inside the diffusion layer. (From Maksimović and Popov[45]).

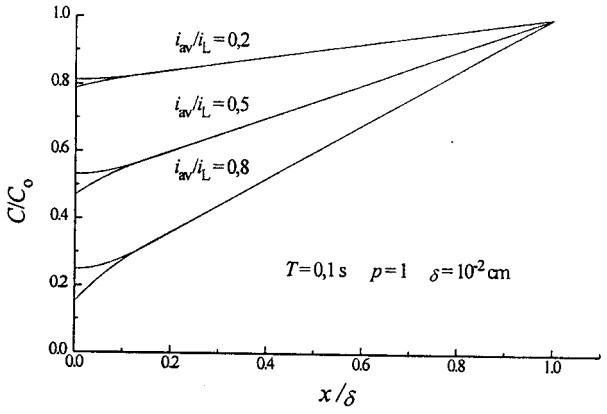

Fig. 15. The effect of the average current density on the concentration distribution inside the diffusion layer. (From Maksimović and Popov[45]).

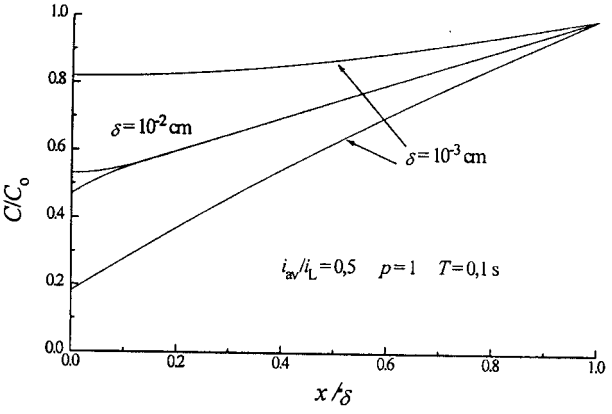

Fig. 16. The effect of the diffusion layer thickness on the concentration distribution inside the diffusion layer. (From Maksimović and Popov[45]).

It can be seen from Fig. 13, that at the lower period of the PC wave, the concentration distribution is closer to that described by Eq. (50) for $T \rightarrow 0$. It can

also be seen from Fig. 14. and Fig. 15, that with other parameters, the same distribution is closer to that given by Eq. (50) at lower p and i_{av} values. Finally, the effect of the diffusion layer thickness is shown in Fig. 16, being the same as in the RC case (see Eq. (22)).

2.3. Alternating current superimposed on direct current

For $i(t)$ given by

$$i(t) = i_{dc} + i_p \sin(\omega t) \tag{51}$$

i.e., for alternating current superimposed on direct current, the solution of the problem is obtained in the form[35,37]

$$c(x,t) = c_0 - \frac{2}{zF\delta} \sum_{k=0}^{\infty} \cos\left[\frac{(2k+1)\pi x}{2\delta}\right] \int_0^t (i_{dc} + i_p \sin(\omega\tau)) \exp[-\lambda_k (t-\tau)]\, d\tau \tag{52}$$

and

$$c(x,t) = c_0 - \frac{2}{zF\delta} \sum_{k=0}^{\infty} \cos\left[\frac{(2k+1)\pi x}{2\delta}\right]$$

$$\left\{\frac{i_{dc}}{\lambda_k}[1 - \exp(-\lambda_k t)] + \frac{i_p}{\lambda_k^2 + \omega^2}\left[\lambda_k \sin(\omega t) - \omega\cos(\omega t) + \omega \exp(-\lambda_k t)\right]\right\} \tag{53}$$

Under steady state conditions, Eq. (53) becomes

$$c(x) = c_0 - \frac{2}{zF\delta} \sum_{k=0}^{\infty} \cos\left[\frac{(2k+1)\pi x}{2\delta}\right]\left\{\frac{i_{dc}}{\lambda_k} + \frac{i_p}{\lambda_k^2 + \omega^2}\left[\lambda_k \sin(\omega t) - \omega\cos(\omega t)\right]\right\} \tag{54}$$

and the surface concentration ($x = 0$) is

$$c_s = c_0 - \frac{2}{zF\delta} \sum_{k=0}^{\infty} \left\{\frac{i_{dc}}{\lambda_k} + \frac{i_p}{\lambda_k^2 + \omega^2}\left[\lambda_k \sin(\omega t) - \omega\cos(\omega t)\right]\right\} \tag{55}$$

Equation (55) can be transformed into a more convenient form:[37]

$$c_s = c_0\left(1 - \frac{i_{dc}}{i_L}\right) - \frac{i_p}{zF(D\omega)^{1/2}} \sin(\omega t - \pi/4) \tag{56}$$

The solution obtained is of the same form as in the case of an unstirred electrolyte,[20,46] *i.e.,* if the condition are given by Eq. (11) it can be written in the form

$$c(t,\infty) = c_0 \tag{57}$$

The maximum difference between the surface concentration and the surface concentration in DC steady state conditions, *i.e.*,

$$c_s = c_0\left(1 - \frac{i_{dc}}{i_L}\right) = c_0 - \frac{\delta\, i_{av}}{zFD} \tag{58}$$

corresponds to the values $\sin(\omega t - \pi/4) = \pm 1$. For $z = 2$, $F = 10^5$ C mol^{-1}, $c_0 = 10^{-4}$ mol cm^{-3} and $\nu = 50$ Hz the term $\dfrac{i_p}{zF(D\omega)^{1/2}}$ can be neglected in Eq. (56) relative to $c_0\left(1 - \dfrac{i_{dc}}{i_L}\right)$, except for the cases of high i_p and $i_{dc} = i_L$.[37]

Hence, at sufficiently small T and not extremely high i_p, c_s in AC will also be given by Eq. (50), implying that at sufficiently high frequencies, the surface concentration is determined by the average current density, regardless of the shape of the current wave.

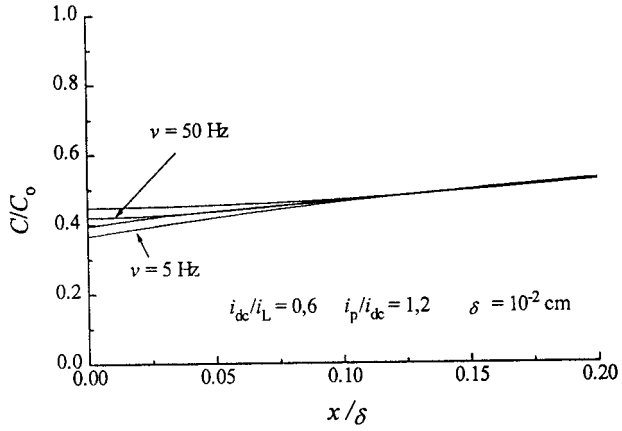

Fig. 17. The effect of the AC frequency on the concentration distribution inside the diffusion layer. (From Maksimović and Popov[47]).

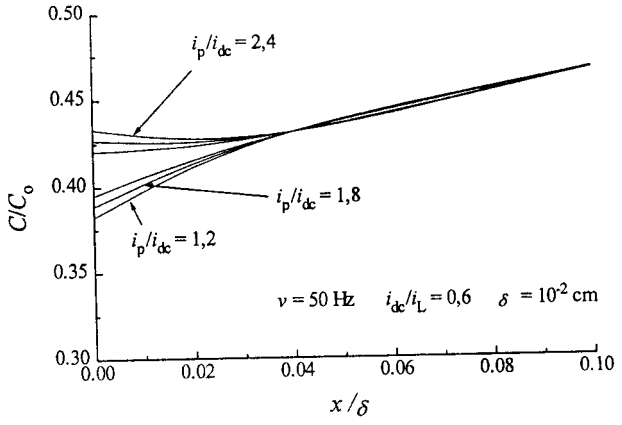

Fig. 18. The effect of the AC amplitude on the concentration distribution inside the diffusion layer. (From Maksimović and Popov[47]).

The concentration distribution inside the diffusion layer, using Eq. (54) and the already used set of parameters ($\delta = 10^{-2}$ cm, $D = 10^{-5}$ cm^2 s^{-1} and $t_0 = 1$ s), is given in Figs. 17– 20 for different AC regimes and $\cos(\omega t - \pi/4) = 0$.[47]

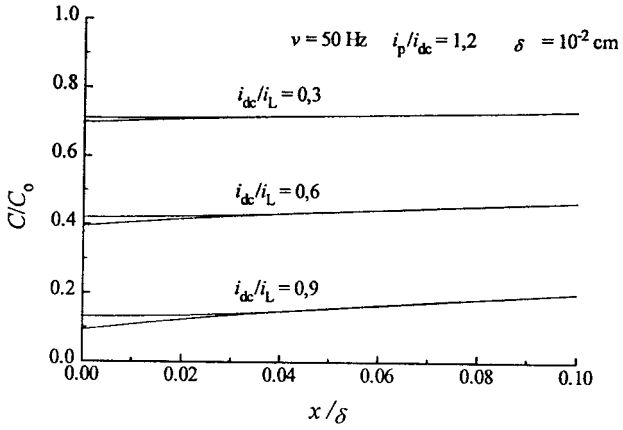

Fig. 19. The effect of the average current density on the concentration distribution inside the diffusion layer. (From Maksimović and Popov[47]).

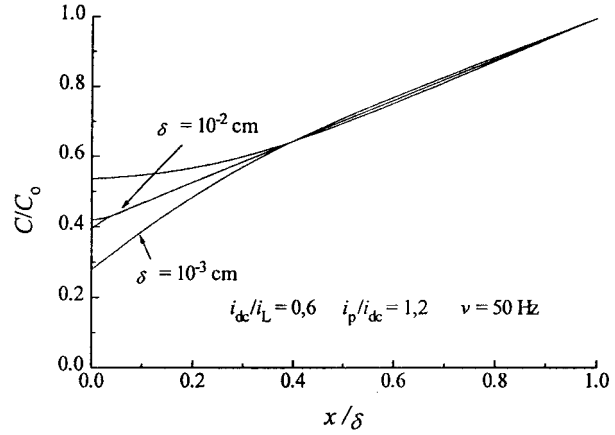

Fig. 20. The effect of the diffusion layer thickness on the concentration distribution inside the diffusion layer. (From Maksimović and Popov[47]).

It can be seen that the effects of frequency, current density and i_p/i_{dc} ratios are practically negligible; the effect of the diffusion layer thickness is more pronounced, being still lower than in the other cases of periodic currents.

3. THE INFLUENCE OF THE CHARGE AND DISCHARGE OF THE ELECTRICAL DOUBLE LAYER

The useful range of frequencies in electrodeposition at a periodically changing rate is known to be limited by mass-transfer effects at low frequencies. At high frequencies, the useful range is limited by the effect of the capacitance of the electrical double layer.[44,48] Details are given in a previous review.[49]

4. THE VALIDITY OF THE MATHEMATICAL MODEL

4.1. Reversing current in the millisecond range

The fact that in the millisecond range, the surface concentration under periodic conditions practically does not vary with time has been experimentally verified. For example, it follows from Eq. (27) that for $i_c = i_a$ and $r = 1$ during RC deposition

$$c_s = c_0 \tag{59}$$

The shape of the RC used and a typical overpotential *versus* time response are shown in Fig. 21 for copper deposition from 0.075 M $CuSO_4$ in 0.5 M H_2SO_4.[50] The current densities and overpotential from these oscillographs, corrected for the ohmic drop, are plotted in Fig. 22. The Tafel lines obtained in this way are similar to those obtained by Mattsson and Bockris[51] in the galvanostatic single-pulse regime for the same system. This is because, at 100 Hz, condition (27) is satisfied and a concentration overpotential does not appear.

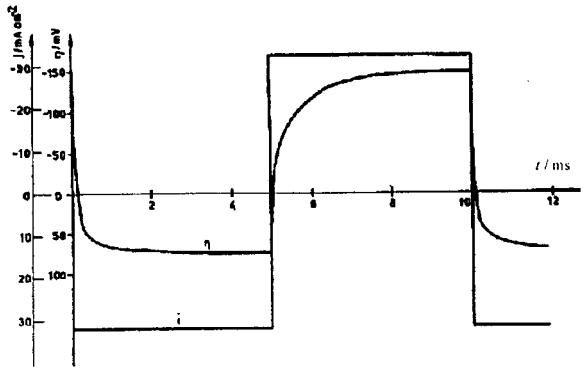

Fig. 21. The shape of the square-wave alternating current and the typical overpotential *versus* time response. Copper electrodeposition from 0.075 M $CuSO_4$ in 0.5 M H_2SO_4. (From Popov *et al.*[50]).

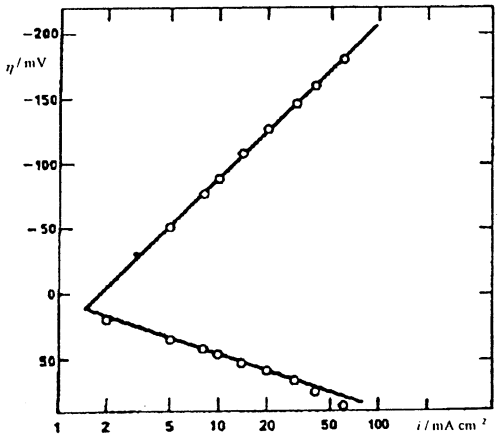

Fig. 22. The cathodic and anodic Tafel lines (obtained from graphs similar to those in Fig. 21) for the $Cu^{2+}|Cu$ system from 0.075 M $CuSO_4$ in 0.5 M H_2SO_4. (From Popov et al. [50]).

4.2. Reversing current in the second range

The mathematical model of RC in the second range can be easily tested for $i_c > i_L$. The solution of Eqs. (9) to (12) for

$$i(t) = i_c \tag{60}$$

is given by[43,52]

$$c_s = c_0 - \frac{i_c \delta}{zFD}\left\{1 - \frac{8}{\pi^2}\sum_{k=0}^{\infty}\frac{1}{(2k+1)^2}\exp\left[-\frac{(2k+1)^2 t}{4t_0}\right]\right\} \tag{61}$$

and the surface concentration of depositing ions for $t \geq t_0$ is given by[43]

$$c_s = c_0 - \frac{i_c \delta}{ZFD}\left\{1 - \frac{8}{\pi^2}\exp\left(-\frac{t}{4t_0}\right)\right\} \tag{62}$$

The maximum amplitude of the current density variation, i_A, corresponding $c_s = 0$ after a deposition time t_c is given by

$$i_A = \frac{i_L}{1 - \frac{8}{\pi^2}\exp\left(-\frac{t_c}{4t_0}\right)} \tag{63}$$

or taking into account $t_c = T/(r+1)$ by

$$i_A = \frac{i_L}{1 - \frac{8}{\pi^2}\exp\left(-\frac{T}{4(r+1)\,t_0}\right)} \tag{64}$$

Substitution of r from Eq. (31) in Eq. (64) and further rearranging gives[53]

$$T = \frac{4\delta^2}{\pi^2 D}\ln\frac{1 - \frac{\pi^2}{16} + \frac{i_L}{i_A}}{\frac{\pi^2}{16}\left(1 - \frac{i_L}{i_A}\right)} \tag{65}$$

In this way the period T of the RC wave and the amplitude current density i_A, which makes the surface concentration at the end of the cathodic pulse zero, are related if the final surface concentration (the end of the anodic pulse) is equal to the initial surface concentration (the beginning of the cathodic pulse) and $i_A \geq i_L$.

Dependencies of overpotential on time were obtained upon application of different RC input waves. The results for the unstirred solution are shown in Figs. 23a – 23c. It can be seen from Fig. 23a that the shape of the overpotential wave does not vary with time after about the first 3 periods, meaning that a steady state periodic response was established. With anodic pulses of shorter duration (Fig. 23b), the overpotential at the end of the cathodic pulses increases, indicating a decrease in the surface concentration. The opposite effect takes place with longer anodic pulse duration (Fig. 23c).

The results for stirred solution are presented at Fig. 23d. Following the same procedure as in the previous case, the RC wave which leads to a steady state periodic response was determined. The shape of the RC wave from Fig. 23d is the same as for the case of unstirred solution, but, due to different hydrodynamic conditions, the period T is quite different.

The T *versus* δ^2 plot shown in Fig. 24. proves that Eq. (65) is valid and that, for metal deposition by RC in the second range, the condition $T/\delta^2 = \text{const.}$ must be fulfilled in order to obtain the same effect on the mass transfer under hydrodynamic conditions, for the same i_A/i_L.

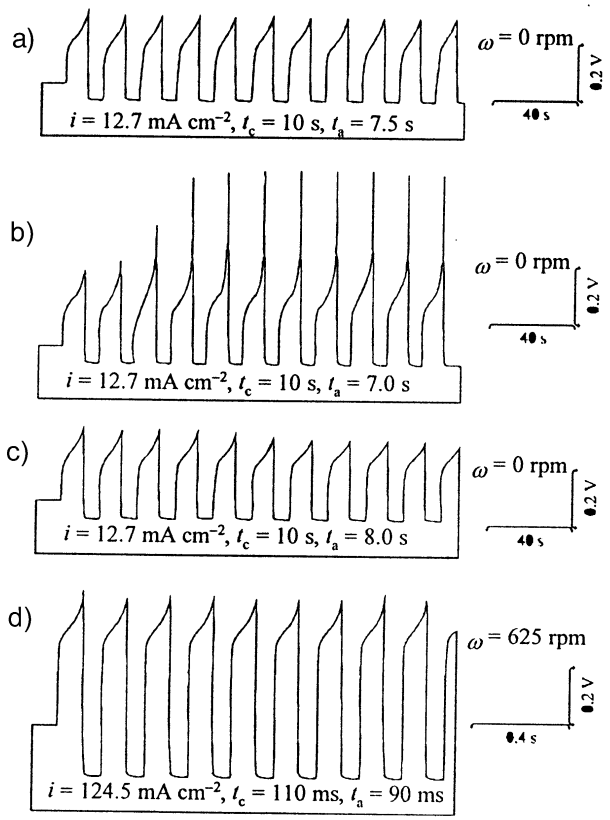

Fig. 23. The dependencies of the overpotential on time, obtained upon application of different RC wave inputs in 0.1 M $CuSO_4$ in 0.5 M H_2SO_4. (From Maksimović *et al.*[54]).

Finally, the current wave with the same i_A and t_c/t_a ratio, but in the millisecond range leads to a potential response characteristic for the dominance of activation control (Fig. 25). The above fact is a continuation of all earlier theoretical predictions.

4.3. Pulsating current

During the pause, under non-current conditions, at frequency values below those of double layer effects, which may, therefore, be neglected, but for which Eq. (44) is valid, the measured potential is equal to the Nernst concentration potential

$$\varphi = \frac{RT}{zF} \ln \frac{c_0}{c_s} \tag{66}$$

Taking into account that

$$c_s = c_0 \left(1 - \frac{i_{av}}{i_L}\right) \tag{67}$$

Eq. (66) can be rewritten in the form

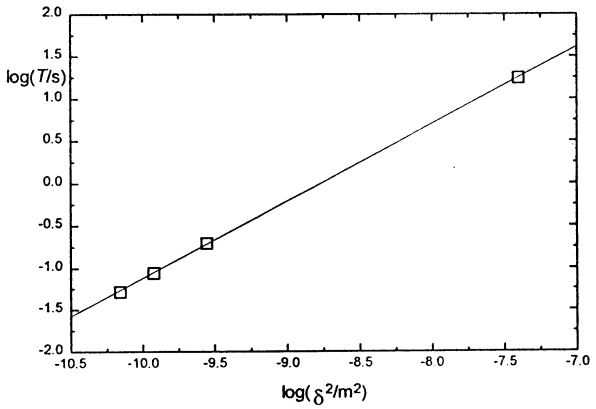

Fig. 24. The dependence of the period of pulsation, T, on the square of the diffusion layer thickness, δ^2 for copper electrodeposition from 0.1 M $CuSO_4$ in 0.5 M H_2SO_4. (From Maksimović *et al.*[54]).

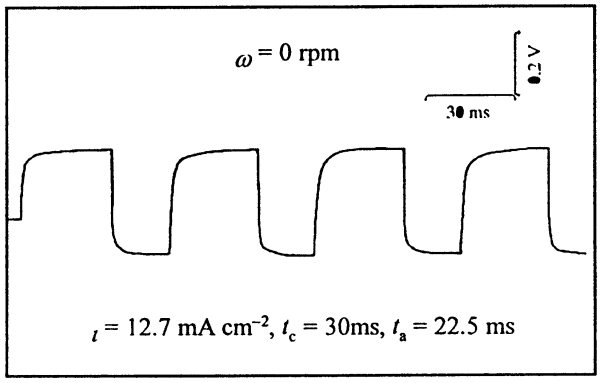

Fig. 25. The potential response to the RC in the millisecond range with the same i_A and t_c/t_a as in Fig 23a. Copper electrodeposition from 0.1 M $CuSO_4$ in 0.5 M H_2SO_4. (From Maksimović *et al.* [54]).

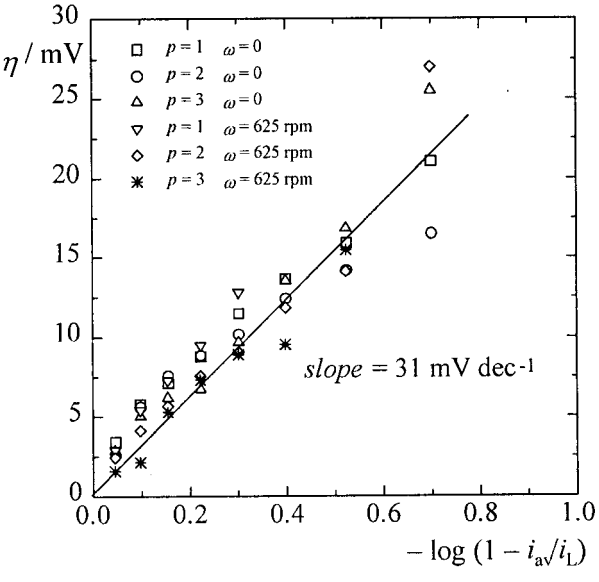

Fig. 26. The Nernst concentration potential at the end of the pause *vs.* log $(1 - i_{av}/i_L)$ in stirred and unstirred solutions (0.1 M $CuSO_4$ and 0.5 M H_2SO_4) for a pulse duration of 50 ms and different pause to pulse ratio. (From Maksimović *et al.* [54]).

$$\varphi = -\frac{RT}{zF}\ln\left(1-\frac{i_{av}}{i_L}\right) \tag{68}$$

The validity of Eq. (68) was tested by determining the concentration in an unstirred and stirred solution as a function of the i_{av}/i_L value. A PC with on period duration of 50 ms and p values of 1,2 and 3 was used. Fig. 26 shows that, in all cases, a straight line with a slope of 31 mV dec^{-1} was obtained. The slope value is very close to 29.5 mV dec^{-1} which is predicted by the Eq. (68), meaning that the mathematical model of PC is operative. This was also proven by considering the overpotentials during the current pulses.[55]

4.4. Pulsating overpotential

In the case of a rectangular pulsating overpotential, $\eta(t)$ as a function of time is given by [56]

$$\eta(t) = \begin{cases} \eta_A, & \text{for } mT < t \le [m + 1/(p+1)]T \\ 0, & \text{for } [m + 1/(p+1)]T < t \le (m+1)T \end{cases} \tag{69}$$

Assuming that the surface concentration is determined by the average current density, the current response to the input overpotential is given by

$$i(t) = i_0\left[\left(1-\frac{i_{av}}{i_L}\right)\exp\left(\frac{\eta(t)}{\eta_{oc}}\right) - \exp\left(\frac{-\eta(t)}{\eta_{oa}}\right)\right] \tag{70}$$

For a sufficiently high η_A, Eq. (70) reduces during the on periods to

$$i_{on} = i_0\left(1-\frac{i_{av}}{i_L}\right)\exp\left(\frac{\eta_A}{\eta_{oc}}\right) \tag{71}$$

and during the off periods to

$$i_{off} = -i_0\frac{i_{av}}{i_L} \tag{72}$$

The average current in PO deposition can easily be determined by

$$i_{av} = \frac{i_0}{p+1}\left[\left(1-\frac{i_{av}}{i_L}\right)\exp\left(\frac{\eta_A}{\eta_{oc}}\right) - p\frac{i_{av}}{i_L}\right] \tag{73}$$

The average overpotential is then given by

$$\eta_{av} = \frac{\eta_{dc}}{p+1} + \frac{\eta_{oc}}{p+1}\ln\left(p+1+p\frac{i_0}{i_L}\right) \tag{74}$$

where

$$\eta_{dc} = \eta_{oc}\ln\frac{i_{av}}{i_0} - \eta_{oc}\ln\left(1-\frac{i_{av}}{i_L}\right) \tag{75}$$

and

$$\eta_{av} = \frac{\eta_A}{p+1} \tag{76}$$

Polarization curves for the average values for copper deposition have been successfully calculated from the stationary polarization curve using Eq. (74)[56] for $i_0 << i_L$, as shown in Fig. 27.

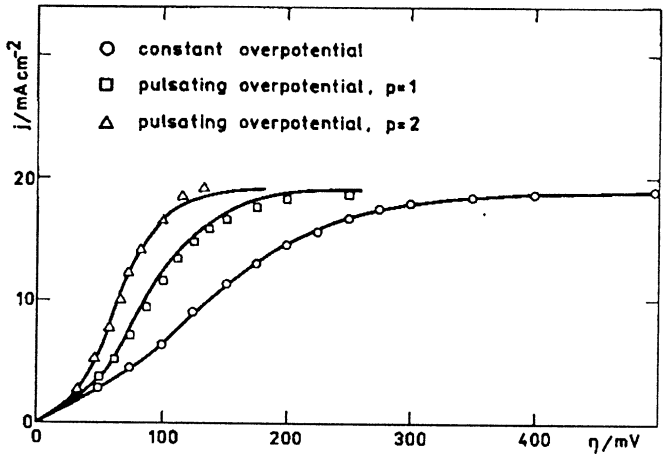

Fig. 27. The stationary polarization curve and the polarization curves of the average values for different pause-to-pulse ratios in a square-wave PO copper electrodeposition from 0.2 M $CuSO_4$ in 0.5 M H_2SO_4. Pulse duration 20 ms. The points represents measured values and the full lines are calculated using Eq. (76) and values from the constant polarization curve. (From Popov *et al.* [56]).

This is a good proof that in PO deposition, the average current density also determines the surface concentration of the depositing ion.

5 . CONCLUSION

The mass-transfer conditions during metal electrodeposition at a periodically changing rate are very important because they determine the morphology of metal deposits just as in the case of electrodeposition at a constant rate. Electrodeposition at a periodically changing rate was described by a common mathematical model and the particular solutions for each type of waveform used are given in the form of time and distance-dependent concentrations inside electrode diffusion layer. It was shown that in all cases of deposition in the millisecond range the surface concentration of depositing ions is constant and determined by the average deposition current density at sufficiently large frequencies of pulsation. At lower frequencies the surface concentration oscillates around the value corresponding to the deposition by the average current density during the constant current deposition. In the case of reversing current deposition in a second range the concentration varies with time in a way that surface concentration at the end of the anodic pulse is close to initial one. All theoretical conclusion are verified by appropriate experiments. The above

solutions are important because they permit to correlate the morphology of deposits with depositing regime, as in the case of constant current deposition.

SUMMARY

The mass-transfer conditions during electrodeposition of metals at a periodically changing rate are considered. The concentration distribution inside the diffusion layer and the surface concentration of depositing ions for pulsating and reversing current and pulsating overpotential are discussed and illustrated by the appropriate experiments. On the basis of the above results, the maximum deposition rates and the effect on the morphology of metal deposits can be elucidated in all cases under consideration.

И З В О Д

ПРЕНОС МАСЕ ТОКОМ ЕЛЕКТРОХЕМИЈСКОГ ТАЛОЖЕЊА МЕТАЛА ПЕРИОДИЧНО ПРОМЕНЉИВОМ БРЗИНОМ

МИОДРАГ Д. МАКСИМОВИЋ и КОНСТАНТИН И. ПОПОВ
Технолошко-металуршки факултет, Универзитет у Београду, п.пр. 3503, 11120 Београд

Размотрени су услови преноса масе током електрохемијског таложења метала периодично променљивом брзином. Расподела концентрације унутар дифузиног слоја и површинска концентрација јона који се таложе дискутоване су и илустроване одговарајућим експериментима за пулсирајућу и реверсну струју и пулсирајућу пренапетост. На основу изнетих резултата могуће је проценити максималну брзину таложења и утицаја на морфологију у свим размотреним случајевима.

(Примљено 2. фебруара 1999)

REFERENCES

1. N.N.Bibikov, *Electrodeposition of Metals by AC*, Mashgiz, Moscow, 1961 (in Russian)
2. J.W.Dini, *Met. Finish.* **61** (1963) 52
3. G.T.Bakhvalov, *New Technology of Electrodeposition of Metals*, Izd. Met., 1966 (in Russian)
4. A.R.Despić, K.I.Popov, *Modern Aspects of Electrochemistry*, No. 7, B.E.Conway and J.O'M.Bockris, Eds., Plenum Press, New York, 1972, p. 199
5. C.C.Wan, H.Y.Cheh, H.B.Linford, *Plating* **61** (1974) 559
6. R.B.Snider, H.Y.Cheh, *Plat. Surf. Finish.* **62** (1975) 786
7. J.Cl.Puippe, N.Ibl, *Oberfläche-Surface* **18** (1977) 205
8. G.Perger, P.M.Robinson, *Met. Finish.* **77** (12) (1979) 17
9. S.Venkatesh, D.T.Chin, *Isr. J. Chem.* **18** (1979) 56
10. N.Ibl, *Surface Technol.* **10** (1980) 81
11. E.Robert, *Oberfläche-Surface* **24** (1983) 413
12. D.Landolt, *Oberfläche-Surface* **25** (1984) 6
13. Yu.M.Polukarov, V.V.Grinina, *Itogi nauki i tehniki (Elektrokhimiya)*, No. 22, Viniti, Moscow, 1985, p. 8
14. A.M.Pesco, H.Y.Cheh, *Modern Aspects of Electrochemistry*, No. 19, B.E.Conway, J.O'M.Bockris and R.E.White, Eds., Plenum Press, New York, 1989, p. 251

15. K.I.Popov, M.D.Maksimović, *Modern Aspects of Electrochemistry*, No. 19, B.E.Conway, J.O'M.Bockris and R.E.White, Eds., Plenum Press, New York, 1989, p. 193
16. K.I.Popov, D.N.Keča, S.I.Vidojković, B.J.Lazarević, V.B.Milojković, *J. Appl. Electrochem.* **6** (1976) 365
17. K.Viswanathan, H.Y.Cheh, *J. Electrochem. Soc.* **126** (1979) 398
18. D.T.Chin, *J. Electrochem. Soc.* **130** (1983) 1657
19. E.Warburg, *Ann. Physik.* **67** (1899) 493
20. F.Krüger, *Z. Phys. Chem.* **45** (1903) 1
21. T.R.Rosebrugh, W.L.Miller, *J. Phys. Chem.* **14** (1910) 816
22. V.I.Chernenko, M.A.Loshkarev, Z.I.Levitin, *Zh. fiz. khim.* **37** (1963) 1015
23. V.I.Chernenko, K.I.Litovchenko, *Elektrokhimiya* **4** (1968) 1452
24. H.Y.Cheh, *J. Electrochem. Soc.* **118** (1971) 551
25. H.Y.Cheh, *J. Electrochem. Soc.* **118** (1971) 1133
26. A.R.Despić, K.I.Popov, *J. Appl. Electrochem.* **1** (1971) 275
27. V.I.Belokon, B.B.Chernov, N.Ya.Kovarskiy, *Elektrokhimiya* **11** (1975) 1655
28. K.Tokuda, H.Matsuda, *J. Electroanal. Chem.* **82** (1977) 157
29. K.Tokuda, H.Matsuda, *J. Electroanal. Chem.* **90** (1978) 147
30. N.N.Alekseenko, S.L.Goldsteyn, D.F.Rakipov, S.P.Raspopin, *Elektrokhimiya* **14** (1978) 676
31. K.Viswanathan, M.A.Farrell Epstein, H.Y.Cheh, *J. Electrochem. Soc.* **125** (1978) 1772
32. K.Viswanathan, H.Y.Cheh, *J. Appl. Electrochem.* **9** (1979) 537
33. K.I.Popov, M.D.Maksimović, B.M.Ocokoljić, B.J.Lazarevic, *Surface Technol.* **11** (1980) 99
34. P.C.Andricacos, H.Y.Cheh, *J. Electroanal. Chem.* **121** (1981) 133
35. S.Venkatesh, D.T.Chin, *J. Electrochem. Soc.* **128** (1981) 2588
36. K.I.Popov, M.D.Maksimović, M.S.Simić, *Surface Technol.* **16** (1982) 209
37. M.D.Maksimović, D.C.Totovski, A.P.Ivic, *Surface Technol.* **18** (1983) 233
38. R.Sethi, D.T.Chin, *J. Electroanal. Chem.* **160** (1984) 79
39. C.Y.Cheng, D.T.Chin, *Am. Inst. Chem. Eng. J.* **30** (1984) 757
40. C.Y.Cheng, D.T.Chin, *Am. Inst. Chem. Eng. J.* **30** (1984) 765
41. A.M.Pesco, H.Y.Cheh, *J. Electrochem. Soc.* **131** (1984) 2259
42. M.D.Maksimović, K.I.Popov, *Zaštita materijala*, **36** (1995) 91
43. K.I.Popov, M.D.Maksimović, *J. Serb. Chem. Soc.* **56** (1991) 25
44. K.I.Popov, M.D.Maksimović, D.C.Totovski, *J. Serb. Chem. Soc.* **50** (1985) 319
45. M.D.Maksimović, K.I.Popov, *Zaštita materijala*, **37** (1996) 45
46. Z.Kovač, *J. Electrochem. Soc.* **118** (1971) 51
47. M.D.Maksimović, K.I.Popov, *Zaštita materijala,* **38** (4) (1997) 8
48. J.Cl.Puippe, *Theory and Practice of Pulse Plating*, J. Cl. Puippe and F. Leaman, Eds., AESFS, Orlando, 1986. Chap. 1
49. M.D.Maksimović, *J. Serb. Chem. Soc.* **60** (1995) 119
50. K.I.Popov, M.D.Maksimović, V.M.Nakić, M.D.Spasojević, *Glasnik Hem. društva Beograd*, **47** (1982) 511
51. B.E.Mattsson, J.O'M.Bockris, *Trans. Farday Soc.* **55** (1959) 1586
52. K.J.Vetter, *Elektrokhimicheskaya Kinetika*, Khimiya, Moskva, 1967
53. J.Cl.Puippe, *Theory and Practice of Pulse Plating*, J.Cl.Puippe and F.Leaman, Eds., AESFS, Orlando, 1986. Chap. 4
54. M.D.Maksimović, S.Gojković, R.M.Stevanović, K.I.Popov, *Bull. Electrochem.* **13** (1997) 413
55. K.I.Popov, M.D.Maksimović, V.M.Nakić, M.D.Spasojević, *Surf. Technol.* **15** (1982) 161
56. K.I.Popov, M.D.Maksimović, S.K.Zečević, M.R.Stojić, *Surf. Technol.* **27** (1986) 117.